

Propagation of Sound Waves through a Linear Shear Layer

James N. Scott*

NASA Lewis Research Center, Cleveland, Ohio

Closed-form solutions are presented for sound propagation from a line source in or near a shear layer. The analysis is exact for all frequencies and is developed assuming a linear velocity profile in the shear layer. This assumption allows the solution to be expressed in terms of parabolic cylinder functions. The solution is presented for a line monopole source first embedded in the uniform flow and then in the shear layer. Solutions are also discussed for certain types of dipole and quadrupole sources. Asymptotic expansions of the exact solutions for small and large values of Strouhal number give expressions which correspond to solutions previously obtained for these limiting cases.

Nomenclature

$A(k)$	= arbitrary coefficient in Eq. (A7)
$B(k)$	= arbitrary coefficient in Eq. (A9)
b	= transformation parameter defined by Eq. (A13)
$C_{\pm}(k)$	= arbitrary coefficients in Eq. (A15)
c_0	= speed of sound, 340.46 m/s
f_j	= arbitrary unit source term in uniform flow region
f_{Tj}	= Fourier transform of f_j
f	= externally applied force
g_j	= arbitrary unit source term in shear layer
g_{Tj}	= Fourier transform of g_j
h	= coordinate of source location in $-y$ direction, m
k_0	= ω/c_0
k_1	= wave number in x direction in region 1, $ko \cos \theta$
k	= wave number in x direction
M	= Mach number in shear layer, U/c_0
M_0	= Mach number of uniform flow, U_0/c_0
$P(y, k)$	= Fourier transform of $p(y, x)$
p	= perturbation pressure, N/m ²
q	= external volume flow source, Eq. (15)
r	= radial coordinate of observation point in cylindrical coordinate system, m
S	= $(\delta\omega/c_0)/M_0$ Strouhal number (reduced frequency)
t	= time, s
U	= velocity in x direction in the shear layer, m/s
U_0	= velocity of uniform flow, m/s
$V(y, k)$	= Fourier transform of $v(y, x)$
v	= perturbation velocity in y direction
x	= coordinate in direction of uniform flow
y	= coordinate \perp to direction of uniform flow
$\gamma_{1,2}$	= defined by Eqs. (A8) and (A10)
$\delta(y)$	= dirac delta function
δ	= shear layer thickness, m
θ	= polar coordinate (polar angle) or direction between line connecting source and observation points and direction of uniform flow
θ_c	= critical angle below which sound waves will not propagate through shear layer
λ	= wavelength
ξ	= transformation variable defined by Eq. (A11)
ρ	= density, 1.23 kg/m ³
ω	= angular frequency

Subscripts

d	= dipole
m	= monopole
q	= quadrupole

Introduction

SOUND waves passing through a shear layer are altered both in amplitude and direction. Hence, an observer situated in the far field on the opposite side of a shear layer from a sound source will, in general, hear sound which differs from that originally produced by the source. Any sound produced by an aircraft engine must pass through a shear layer or combination of shear layers. Consequently, a thorough understanding of this phenomenon is essential for determining the far-field sound pressure amplitude directivity generated by an aircraft engine in flight. Such knowledge is also necessary for developing adequate correction procedures for data from open-jet anechoic wind tunnels used for simulating flight effects on noise sources.

There have been several studies of the effect of relative motion between two media on the propagation of sound waves. Ribner¹ and Miles² independently investigated plane waves impinging on a velocity interface between two moving streams. Gottlieb³ studied a sound source near a velocity discontinuity. He obtained far-field solutions by evaluating the exact sound field integrals by the method of stationary phase. Slutsky and co-workers⁴⁻⁶ extended Gottlieb's analysis to include quadrupole sources embedded in the mean flow. Their analyses were developed for the sources situated in an axisymmetric slug flow. Graham and Graham⁷ treated the propagation of plane waves through a finite shear layer. The same authors⁸ later investigated the effect of a finite shear layer on sound waves from a point source. They obtained velocity potential solutions by means of a series expansion about a singular point and presented results for very low frequencies with acoustic wavelengths much greater than the shear layer thickness.

Goldstein^{9,10} obtained solutions for low-frequency sound from multipole sources in axisymmetric shear flows with arbitrary velocity profiles. The results of his analysis show how the mean flow affects the radiation pattern from the sources. Balsa¹¹ gives expressions for pressure fields of various high-frequency convected sources embedded in a unidirectional sheared flow. The expressions include the simultaneous effects of fluid and source convection and refraction. Those results are for axisymmetric flows with arbitrary velocity profiles.

The next step in determining the effect of a shear layer upon sound propagation is to obtain analytic solutions for the far-field pressure for the entire acoustic frequency range. This has been accomplished in the present investigation¹² by using an exact analytical solution obtained by Goldstein and Rice¹³ not

Presented as Paper 78-196 at the AIAA 16th Aerospace Sciences Meeting, Huntsville, Ala., Jan. 16-18, 1978; received March 1, 1978; revision received Sept. 21, 1978. Copyright © American Institute of Aeronautics and Astronautics, Inc., 1978. All rights reserved.

Index category: Aeroacoustics.

*Aerospace Engineer. Member AIAA.

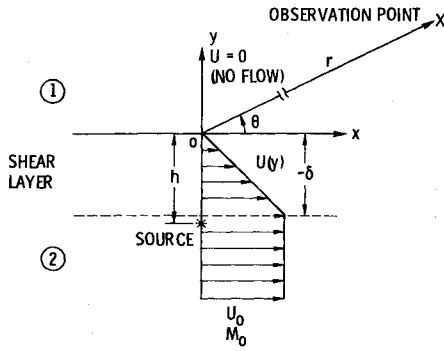


Fig. 1 Schematic of simplified shear layer used in analysis.

only for a monopole source in a uniform flow near a linear shear layer, but for dipole and quadrupole sources as well. This analysis is further extended to the case in which the source is embedded in the shear layer for a monopole, and a quadrupole-type source for the entire frequency spectrum.

Analysis

A simplified formulation of this problem is based on the flow geometry shown in Fig. 1 where a medium moving with a uniform velocity U_0 (region 2) and a medium at rest (region 1) are separated by a single shear layer having a linear velocity profile. The no-flow case is used on one side of the shear layer for simplicity, and the solutions can be easily extended to the more general case of finite uniform flow on both sides. Cases will be considered in which a line source is located in the uniform flow and in the shear layer.

The governing equations for sound propagation in each of these regions may be found in Ref. 14 (p. 10) and are given in terms of acoustic pressure as follows:

- 1) In the no-flow region, $U=0$ (region 1),

$$\nabla^2 p_1 = \frac{1}{c_0^2} \frac{\partial^2 p_1}{\partial t^2} \quad (1)$$

- 2) In the uniform flow region $U=U_0$ (region 2),

$$\nabla^2 p_2 - \frac{1}{c_0^2} \frac{D_0^2}{Dt^2} p_2 = f_j \quad j=1,2 \quad (2)$$

where

$$\frac{D_0}{Dt} \equiv \frac{\partial}{\partial t} + U_0 \frac{\partial}{\partial x}$$

and

$$f_j = \begin{cases} \delta(x)\delta(y+h)e^{i\omega t} & j=1 \\ 0 & j=2 \end{cases}$$

accounts for the presence ($j=1$) or absence ($j=2$) of the source (of unit strength) in the uniform flow.

- 3) In the shear layer,

$$\frac{D}{Dt} \left(\nabla^2 p - \frac{1}{c_0^2} \frac{D^2}{Dt^2} p \right) - 2U' \frac{\partial^2 p}{\partial x \partial y} = g_j \quad j=1,2 \quad (3)$$

where the prime denotes differentiation with respect to y ,

$$\frac{D}{Dt} \equiv \frac{\partial}{\partial t} + U \frac{\partial}{\partial x}$$

and

$$g_j = \begin{cases} 0 & j=1 \\ \frac{D}{Dt} [\delta(x)\delta(y+h)e^{i\omega t}] & j=2 \end{cases}$$

accounts for the absence ($j=1$) or presence ($j=2$) of the source in the shear layer.

The relationship between the transverse particle velocity and the acoustic pressure is given by

$$\rho_0 \left(\frac{Dv}{Dt} \right) = - \frac{\partial p}{\partial y}$$

The linear velocity profile in the shear layer is given by

$$U(y) = -U_0 y / \delta$$

For the boundary conditions, we have the acoustic radiation condition which requires outward propagating waves at $y = \pm \infty$. At the edges of the shear layer we require continuity of pressure

$$p = p_1 \text{ at } y=0 \text{ and } p = p_2 \text{ at } y=-\delta \quad (4)$$

and continuity of particle displacement which can be expressed in terms of the transverse perturbation velocity (since there is no slip)

$$v = v_1 \text{ at } y=0, \text{ and } v = v_2 \text{ at } y=-\delta \quad (5)$$

The method used to obtain the solution to this system of equations is outlined in the Appendix. The result, given here in cylindrical coordinates, is the following expression for the far-field pressure directivity for a line monopole source located in the uniform flow:

$$p_{lm} = \frac{-2\sqrt{(2\delta/r - rM_0 \cos\theta)} \sin\theta / [(b+1/2)\Gamma(b-1/2)]}{G^* - R^* + -R^* - G^*} \times \exp -i \frac{\omega}{c_0} \{ \sqrt{(1-M_0 \cos\theta)^2 - \cos^2\theta} (-\delta+h) + r + c_0 t \} \quad (6)$$

where

$$G^* \pm = \left(i \frac{\omega}{c_0} \right)^{-1} G^\pm = \{ (1-M_0 \cos\theta) + \sqrt{(1-M_0 \cos\theta)^2 - \cos^2\theta} \} U(b-1, \pm \xi_2) + \{ (1-M_0 \cos\theta) - \sqrt{(1-M_0 \cos\theta)^2 - \cos^2\theta} \} \times (b-1/2) U(b+1, \pm \xi_2) \quad (7)$$

and

$$R^* \pm = \left(i \frac{\omega}{c_0} \right)^{-1} R^\pm = (1-\sin\theta) U(b-1, \pm \xi_1) + (1+\sin\theta) (b-1/2) U(b+1, \pm \xi_1) \quad (8)$$

The frequency is defined in terms of Strouhal number as follows. Recall that

$$b = \frac{k}{2iM'} = i \frac{\delta(\omega/c_0)}{2M_0} \cos\theta$$

and that

$$\xi = \sqrt{\frac{2i}{M'k}} \left(\frac{\omega}{c_0} - kM \right) = \sqrt{\frac{2i(\omega/c_0)\delta}{M_0 \cos\theta}} (1 - M \cos\theta)$$

where $k = k_1 = k_0 \cos\theta$ was used.

Note that $\delta(\omega/c_0)/M_0$ is a nondimensional group of parameters that occurs several places in the pressure expression. Hence, we define the Strouhal number

$$S = \delta(\omega/c_0)/M_0 \quad (9)$$

Then,

$$b = \frac{1}{2} i S \cos \theta$$

and

$$\xi = \sqrt{\frac{2iS}{\cos \theta}} (1 - M \cos \theta)$$

This Strouhal number is essentially a comparison of the shear layer thickness to the convective wavelength, and is referred to as a nondimensional frequency.

Now, placing the source in the shear layer, ($j=2$, $f_{T2}=0$, $g_{T2}=(1/2\pi)\delta(y+h)$) in Eqs. (A2) and (A3) and following exactly the same procedure yields the far-field expression for acoustic pressure

$$p_{lm} = \left[\frac{i}{2\pi(\omega/c_0)r} \right]^{1/2} \frac{(-isin\theta)}{[1 - (h/\delta)M_0 \cos \theta]^2} \times \left\{ \frac{P^+(\xi_h)G^{*-} - P^-(\xi_h)G^{*+}}{G^{*-}R^{*+} - G^{*+}R^{*-}} \right\} e^{-i(\omega/c_0)r + i\omega t} \quad (10)$$

where

$$\xi_h = \sqrt{\frac{2i}{M^*k}} \left(\frac{\omega}{c_0} - k \frac{h}{\delta} M_0 \right) \quad (11)$$

It is noted that when the source is placed at the uniform flow edge of the shear layer, in which case $h=\delta$ and $\xi_2=\xi_h$, Eq. (10) becomes equal to Eq. (6). Both Eqs. (6) and (10) reduce to the same special result regardless of source location when the line between the source and observer is oriented at 90 deg to the flow direction, i.e., $\theta=90$ deg in Eqs. (6) and (10). This result is

$$p_{lm} \Big|_{\theta=90 \text{ deg}} = \left[\frac{1}{8\pi i(\omega/c_0)r} \right]^{1/2} e^{-i(\omega/c_0)(h-2\delta+r) + i\omega t} \quad (12)$$

This also agrees with Gottlieb's result³ at $\theta=90$ deg when the shear thickness δ is set equal to zero.

Approximate Solutions for Limiting Cases of Low and High Frequency

When considering the far-field pressure for limiting values of frequency, it is actually limiting values of nondimensional frequency or Strouhal number [defined by Eq. (9)] which are of interest. Careful examination of the far-field pressure equations [Eqs. (6) and (10)] along with the definitions of b and ξ reveals the strong dependence of the pressure upon Strouhal number. This dependence comes about through the parabolic cylinder functions which can be evaluated for small or large arguments by means of appropriate asymptotic expansions found in Refs. 15 and 16. The parabolic cylinder functions appear only through $A(k)$ as evaluated for $k=k_j=\omega/c_0 \cos \theta$. By evaluating these expressions for the limiting cases of very small and very large values of the Strouhal number the approximate expressions for the far-field pressure will be obtained. These approximate expressions for the far-field pressure can also be obtained by solving the differential equations asymptotically for arbitrary velocity profiles using methods discussed in Sec. 6.7.1 of Ref. 14.

By replacing the parabolic cylinder functions in Eqs. (6) and (10) with their asymptotic expansions¹⁵ for small arguments, the low-frequency approximations for far-field pressure are obtained. Replacing the parabolic cylinder functions with their asymptotic expansions^{15,16} for large arguments gives the approximate high-frequency expressions for the far-field pressure. The results for both cases are given in Ref. 12.

Multipole Sources

This analysis can be extended to multipole sources located either in the uniform flow or in the shear layer. For a

multipole line source located in the uniform flow region, the far-field pressure may be obtained by differentiating the monopole solution with respect to source location.¹² Since the source location is only dependent upon the transverse coordinate direction (y direction) only lateral multipole sources will be of interest here. Thus, far-field pressure due to a lateral line dipole source in the uniform flow is the first derivative with respect to transverse source location (h) of the monopole expression [Eq. (6)]:

$$p_{ld} = \frac{\partial p_{lm}}{\partial h} = -\frac{\omega}{c_0} p_{lm} \sqrt{\cos^2 \theta - (1 - M_0 \cos \theta)^2} \quad (13)$$

The lateral line quadrupole expression is obtained by differentiating the monopole expression [Eq. (6)] twice with respect to transverse source location (h).

$$p_{lq} = \frac{\partial^2 p_{lm}}{\partial h^2} = \left(\frac{\omega}{c_0} \right)^2 p_{lm} [\cos^2 \theta - (1 - M_0 \cos \theta)^2] \quad (14)$$

To obtain far-field pressure solutions for multipole sources located in the shear layer, the equation for wave propagation in a transversely sheared mean flow must be considered. This is given in Chap. 1 of Goldstein¹⁴ in a general form as:

$$\begin{aligned} \frac{D}{Dt} \left(\nabla^2 p - \frac{1}{c_0^2} \frac{D^2}{Dt^2} p \right) - 2 \frac{dU}{dy} \frac{\partial^2 p}{\partial x \partial y} \\ = \frac{D}{Dt} \nabla \cdot \mathbf{f} - 2 \frac{dU}{dy} \frac{\partial f_y}{\partial x} - \rho_0 \frac{D^2}{Dt^2} q \end{aligned} \quad (15)$$

where \mathbf{f} is an externally applied volume force arising from the momentum equation and q is an external volume flow source within the fluid which arises from the continuity equation. If the volume flow source is put equal to zero (i.e., no mass is added to the flow) the two remaining terms on the right-hand side of Eq. (15) are due to the externally applied force \mathbf{f} . Goldstein¹⁴ shows that in flows with no mean velocity an external force behaves as a volume dipole source of strength \mathbf{f} .

Now a dipole source is not uniquely defined in a transversely sheared mean flow. If we want to extend its definition so that its strength still coincides with an external force we can define it so that \mathbf{f} on the right-hand side of Eq. (15) is the strength of a general dipole. Similarly, a quadrupole can be defined so that it corresponds to an external stress. This is done by replacing \mathbf{f} with $\nabla \cdot \mathbf{f}$ where \mathbf{f} is now a tensor. Hence, in particular the source term representing a lateral quadrupole of strength \mathbf{f} in the transverse direction is

$$\frac{D_0}{Dt} \frac{\partial^2 \mathbf{f}}{\partial y^2} - 2 \frac{dU}{dy} \frac{\partial^2 \mathbf{f}}{\partial x \partial y}$$

Hence, the solution to Eq. (15) with $q=0$ can be obtained by differentiating the monopole solution with respect to source location h , once for the dipole (associated with the force vector) and twice for the quadrupole (associated with the stress tensor).

Only the more interesting quadrupole result will be given here.

$$p_q = p_{lm} \left\{ \frac{2(M_0 \cos \theta / \delta)}{(1 - (h/\delta)M_0 \cos \theta)} + i \left(\frac{\omega}{c_0} \right)^2 \left[\left(1 - \frac{h}{\delta} M_0 \cos \theta \right)^3 - \cos^2 \theta \left(1 - \frac{h}{\delta} M_0 \cos \theta \right) \right] \right\} \quad (16)$$

where p_{lm} is given by Eq. (10). This expression gives the far-field pressure for a point lateral quadrupole source located in the shear layer.

Inspection of Eq. (16) indicates that the first term inside the braces will dominate at low frequencies, while the second

term, containing $(\omega/c_0)^2$, will dominate at high frequencies. Thus, the product of these respective terms with the low- and high-frequency approximations for p_l will give the low- and high-frequency approximations for the far-field quadrupole pressure pattern, respectively.

The low-frequency approximation is

$$p_{lq} = \frac{2[(M_0/\delta)\cos\theta]^2}{[1 - (h/\delta)M_0\cos\theta]} p_{lm} \quad (17)$$

where p_{lm} is given by the low-frequency approximation for the monopole source in the shear layer. The high-frequency approximation is

$$p_{lq} = i(\omega/c_0)^2 \{ [1 - (h/\delta)M_0\cos\theta]^3 - \cos^2\theta [1 - (h/\delta)M_0\cos\theta] \} p_{lm} \quad (18)$$

where p_{lm} is given by the approximate high-frequency solution for the monopole source in the shear layer. The details of the preceding analysis may be found in Ref. 12.

Results and Discussion

The far-field pressure pattern for sound radiating from a given type of point source in a uniform flow or a linear shear layer may be controlled by a number of different factors. Among these are Mach number of the uniform flow, frequency of the sound, shear layer thickness, and source location with respect to the shear layer. The effects of varying these parameters are determined from the appropriate pressure solutions given in the preceding section. It should be noted that three-dimensional effects and turbulent scattering were ignored in obtaining the pressure expressions.

The sound pressure field was calculated by programming the various pressure expressions using standard Fortran techniques. The parameter r has been normalized to 0.305 m. The parabolic cylinder functions occurring in the exact pressure expressions were calculated using a computer program which was originally developed in connection with other research being performed at NASA Lewis Research Center. This program was capable of calculating up to 80 terms in the series for parabolic cylinder functions with complex arguments. At higher frequencies this proved to be inadequate. However, at the frequencies where computational difficulties were encountered with the exact solution, the approximate expressions had already shown good agreement with the exact solutions. These calculations were made using single precision arithmetic which gave nine significant decimal digits. The directivity calculations were made at 5-deg intervals.

Figures 2-6 show pressure level referenced to ρc_0^2 [i.e., pressure level = $10 \log_{10} |p_l/\rho c_0^2|^2$] plotted against $\theta' = 180^\circ - \theta$, where θ is the angle from the positive x axis (downstream flow direction). These curves are for a source of unit strength, a uniform flow Mach number of 0.8, and a shear layer thickness of 0.153 m. The plots compare the exact and approximate calculations derived in the previous sections as indicated in the various figures.

Source in the Uniform Flow

Figure 2 shows results for a source in the uniform flow. When treating a point source located in the uniform flow, the source is considered to be within a few wavelengths of the shear layer. If the source is many wavelengths from the shear layer the problem degenerates to the plane wave case already treated by Graham and Graham.⁷

One of the most significant characteristics of the pressure pattern in Fig. 3 is the designated "zone of silence." This region is determined by the quantity $\sqrt{(1 - M_0\cos\theta)^2 - \cos^2\theta}$ which appears in G^* [Eq. (7)] as well as in the exponent of the far-field pressure expression [Eq. (6)]. The angle at which

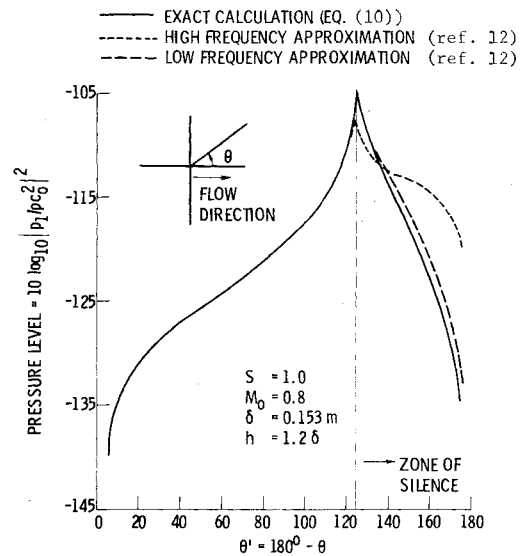


Fig. 2 Comparison of exact and approximate pressure expressions for a monopole source in a uniform flow.

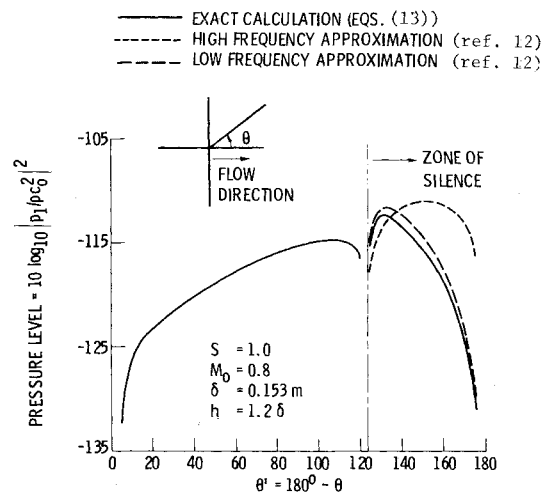


Fig. 3 Comparison of exact and approximate pressure expressions for a transverse dipole source in the uniform flow.

this square root becomes zero is referred to as the critical angle and is defined by

$$\theta_c = \cos^{-1} \left(\frac{1}{1 + M_0} \right)$$

This is the smallest angle θ that the transmitted wave can make with the x axis. Note that this angle is completely controlled by the Mach number of the uniform flow. The "zone of silence" is defined as the region where θ is less than θ_c . In this region the preceding square root term acts as an exponential damping factor. Hence, the "zone of silence" is actually a zone of attenuated sound propagation. For the region in which θ is greater than θ_c the square root term contributes only to the phase of the sound wave and no longer affects the amplitude.

The far-field pressure patterns for dipole and quadrupole sources in the uniform flow are shown in Figs. 3 and 4. These far-field pressure patterns also exhibit a well-defined zone of silence. However, rather than peaking at the critical angle the pressure level goes to $-\infty$ due to the fact that the preceding term is a multiplicative factor in the pressure expressions [Eqs. (13) and (14), respectively] which therefore go to zero at θ_c in each case.

The curves shown in Figs. 2-4 are all for a Strouhal number of 1, which means that the convective wavelength is ap-

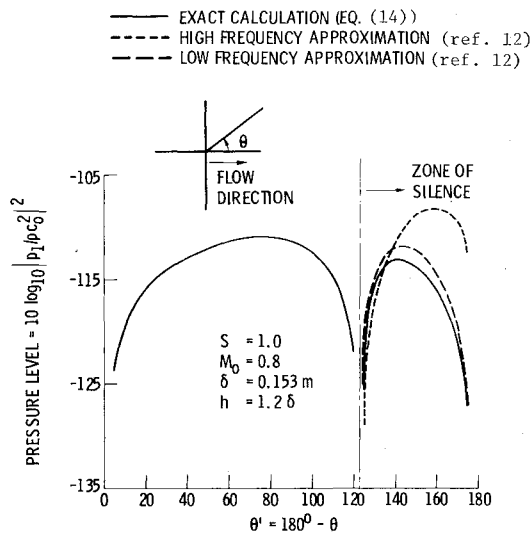


Fig. 4 Comparison of exact and approximate pressure expressions for a transverse quadrupole source in the uniform flow.

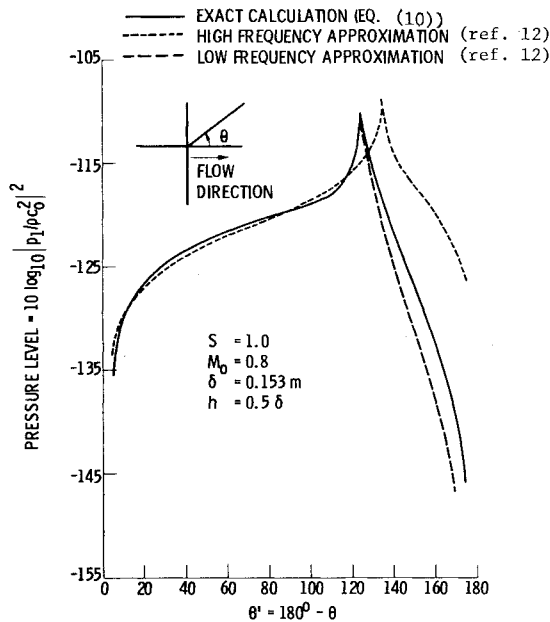


Fig. 5 Comparison of exact and approximate pressure expressions for a monopole source in the shear layer.

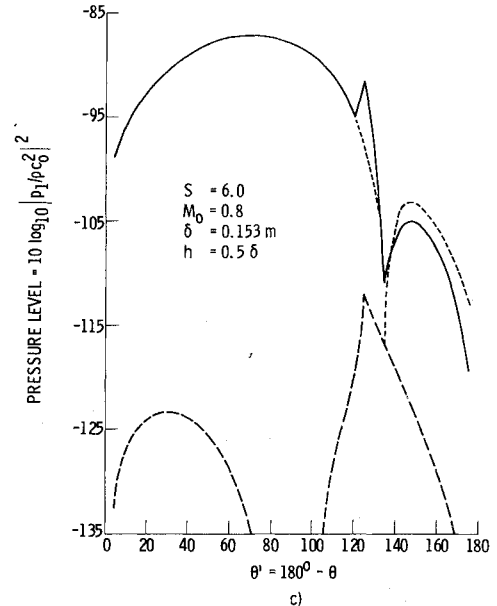
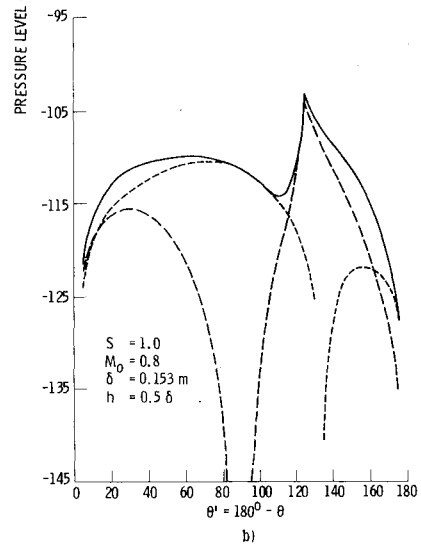
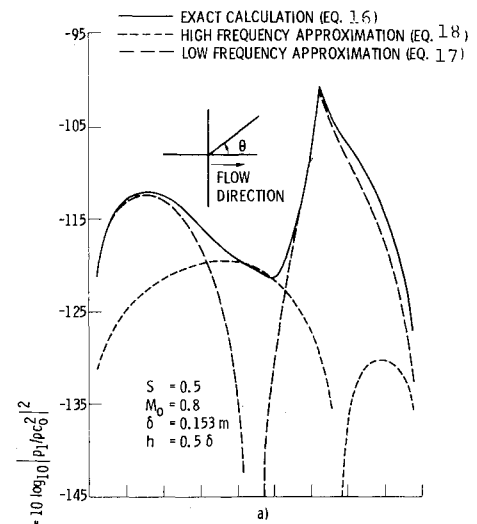


Fig. 6 Comparison of exact and approximate pressure expressions for a transverse quadrupole source in the shear layer.

Source in the Shear Layer

The sound radiation field due to a volume flow source embedded in the shear layer is similar in nature to that of a monopole source located in the uniform flow. A typical radiation pattern for a monopole source in the shear layer is shown in Fig. 5 for a Strouhal number of 1.

proximately equal to the shear layer thickness. Additional calculations were made for Strouhal numbers ranging from 0.25 up to about 6.0. For Strouhal numbers much above 3.0 the computer program for calculating the parabolic cylinder functions encountered computational difficulties for angles near 90 deg. Hence, the exact expression for the sound field is reliable only for certain regions of the sound field at higher frequencies. Outside of the zone of silence, both of the approximate calculations agree with the exact result over the range of Strouhal numbers considered. This behavior indicates that neither the radiation pattern nor the method of calculation are particularly sensitive to frequency outside of the zone of silence. This corresponds to the assertion of previous researchers^{7,8} that the shear layer thickness has essentially no effect on the sound radiation pattern except inside the zone of silence ($\theta < \theta_c$). These characteristics carry over directly to the dipole and quadrupole calculations.

Finally, note that the pressure level tends to $-\infty$ at $\theta = 0$ and 180 deg. This corresponds to zero pressure at these angles. This is attributed to the cancellation of incident waves by reflected waves at small incidence angles. This is what Gottlieb³ refers to as the "Lloyd's Mirror Effect."

For the source in the shear layer there still appears to be a zone of silence again determined by $\sqrt{(1 - M_0 \cos \theta)^2 - \cos^2 \theta}$ for the exact and low-frequency results; however, it enters the pressure expression¹² only through the coefficients of the parabolic cylinder functions given by $G^* \pm$ [Eq. (7)] and does not enter directly into the exponent of the exact pressure equation or the low-frequency result. Hence, there is no exponential damping factor in either of these equations. However, the combination of algebraic terms:

$$\frac{(1 - M_0 \cos \theta)^2}{[1 - (h/\delta) M_0 \cos \theta]^2} \times \sin \theta / [(1 - M_0 \cos \theta)^2 \sin \theta + \sqrt{(1 - M_0 \cos \theta)^2 - \cos^2 \theta}]$$

appearing in the low-frequency pressure expression¹² results in a rapid dropoff of the sound levels for angles less than $\theta_c = \cos^{-1} 1/(1 + M_0)$. This behavior is much like the exponential damping in the zone of silence at high frequencies or when the source is in the uniform flow. It should be noted that this rather remarkable feature is independent of frequency, while the exponential damping factors found in the high-frequency approximation for the source in the shear layer and in all results for the source in the uniform flow do depend on frequency.

The peak in the low-frequency approximation curve occurs at θ_c (i.e., when the square root in the denominator of the second factor is zero). As θ decreases below θ_c , the denominator of the second factor approaches 1 (i.e., the square root), while $\sin \theta$ approaches zero, thus causing the decrease in sound level as θ approaches zero. At angles near 90 deg $\sin \theta$ is near 1, causing the sound level to "flatten out" in this region.

The square root $\sqrt{(1 - M_0 \cos \theta)^2 - \cos^2 \theta}$ does not appear in the high-frequency approximation.¹² However, this approximation does contain the $\sqrt{(1 - (h/\delta) M_0 \cos \theta)^2 - \cos^2 \theta}$ both in the denominator and in the exponent. Hence, this square root determines a "critical angle" for the high-frequency expression given by

$$\theta_{c_{hf}} = \cos^{-1} \frac{1}{[1 + (h/\delta) M_0]}$$

Note that $(h/\delta) M_0$ is the local Mach number of the flow at the source location in the shear layer. This accounts for the fact that the peaks for the high-frequency approximation occur at slightly different angles than the peaks of the exact and low-frequency curves.

It should be noted that both of the square root expressions arise originally from the expression $\sqrt{k^2 - (\omega/c_0 - kM)^2} = i(\omega/c_0) \sqrt{(1 - M \cos \theta)^2 - \cos^2 \theta}$. Hence, the square root is zero at branch points of the complex k plane and as shown earlier these points determine "critical angles." It is at these points that the high-frequency expansion breaks down.

The idea of a dipole source or a quadrupole source (or for that matter any other order multipole source) in a transversely sheared mean flow is rather vague since there is no unique way of defining such a source. In obtaining Eqs. 16-18 these sources are defined so that they correspond to an externally applied force and an externally applied stress, respectively. The curves shown in Fig. 6 are for the quadrupole source located at the center of the shear layer, a mean flow Mach number of 0.8, and Strouhal numbers of 0.5, 1.0, and 6.0, respectively.

The exponential damping is most easily seen in the high-frequency approximation.¹² However, this feature is not as pronounced as might be expected. This is because of a masking resulting from the coefficient in Eq. (18).

One further point of significance which applies in general to this type of quadrupole is that the high-frequency approximation [Eq. (18)] resembles the exact expression for a

quadrupole in the uniform flow [Eq. (14)] multiplied by a Doppler factor $(1 - h/\delta M_0 \cos \theta)$, where the Mach number in each case is that of the flow at the source location.

Summary and Conclusion

An analysis has been developed for calculating the far-field acoustic pressure for sound waves propagating through a linear shear layer. The sound waves are produced by a line source either located near the shear layer in a uniform flow or located in the shear layer itself. Closed-form analytic expressions for the far-field pressure have been obtained for several different types of sources (i.e., monopole, dipole, etc.). The definitions of these sources depend upon whether the source is located in the uniform flow or in the shear layer. Approximate expressions were obtained for limiting cases of high and low frequencies for each type of source. These approximate expressions give very good agreement with the exact result for their respective limiting cases.

The exact pressure expression for a monopole source reduces to previously known results for such special cases as zero shear layer thickness, propagation of the sound waves perpendicular to the flow direction, and plane waves propagating through a velocity discontinuity. The exact expressions for multipole sources in the uniform flow are simple extensions of the monopole result. The expression for the monopole or volume flow source in the shear layer becomes identical with the monopole expression in the uniform flow when the source is placed at the edge of the shear layer. The quadrupole source solution in the shear layer is an extension of the monopole solution in the shear layer. Consequently, all of the pressure expressions developed here can be reduced to known results for special limiting cases, thus providing a check for the analysis. Hence, analytic expressions have been developed for calculating the sound field due to various types of line sources located in a uniform flow or in a shear layer for the entire acoustic frequency spectrum. The asymptotic expansions of these exact expressions for the limiting cases of low and high frequency correspond to results presented elsewhere for shear layers of arbitrary velocity profiles.

Appendix

The system of equations and boundary conditions given by Eqs. (1-5) is solved by the following method. A more detailed discussion of this analysis is presented in Ref. 12.

Assuming a simple harmonic time dependence and applying the Fourier transforms

$$P(y, k) = \frac{e^{-i\omega t}}{2\pi} \int_{-\infty}^{\infty} p(x, y) e^{ikx} dx$$

$$V(y, k) = \frac{e^{-i\omega t}}{2\pi} \int_{-\infty}^{\infty} v(x, y) e^{ikx} dx$$

$$\frac{1}{2\pi} \int_{-\infty}^{\infty} \delta(x) e^{ikx} dx = \frac{1}{2\pi}$$

gives the following system of second-order ordinary differential equations and boundary conditions.

In region 1

$$P_1'' + \left[\frac{\omega^2}{c_0^2} - k^2 \right] P_1 = 0 \quad (A1)$$

In region 2

$$P_2'' + \left[\left(\frac{\omega}{c_0} - M_0 k \right)^2 - k^2 \right] P_2 = f_{Tj} \quad j=1, 2 \quad (A2)$$

In the shear layer

$$P'' - \frac{2M'k}{(kM - \omega/c_0)} P' + \left[\left(kM - \frac{\omega}{c_0} \right)^2 - k^2 \right] P = g_{Tj} \quad j=1,2 \quad (\text{A3})$$

where

$$P' = -i\rho_0 c_0 \left(\frac{\omega}{c_0} - kM \right) V \quad (\text{A4})$$

with the boundary conditions

$$P = P_1; \quad V = V_1 \quad \text{at } y=0 \quad (\text{A5})$$

$$P = P_2; \quad V = V_2 \quad \text{at } y=-\delta \quad (\text{A6})$$

The solution of this system will depend on whether the source is located in the uniform flow or in the shear layer. However, the procedure is the same in either case.

The solution of Eq. (A1) in the no-flow region that satisfies the radiation condition has the form

$$P_1 = A(k) e^{-\gamma_1 y} \quad (\text{A7})$$

where

$$\gamma_1 = \sqrt{k^2 - (\omega/c_0)^2} \quad (\text{A8})$$

When the source is in the uniform flow region $j=1$; $f_{T1} = \frac{1}{2}\pi\delta(y+h)$, $g_{T1}=0$ the solution to Eq. (A2) that satisfies the radiation condition has the form

$$P_2 = B(k) e^{\gamma_2 y} + \frac{I}{4\pi\gamma_2} e^{-\gamma_2(y+h)} \quad (\text{A9})$$

where

$$\gamma_2 = \sqrt{k^2 - (\omega/c_0 - kM_0)^2} \quad (\text{A10})$$

The assumption of a linear velocity profile in the shear permits use of the solution obtained by Goldstein and Rice¹³ which expresses the acoustic pressure in the shear layer in terms of the parabolic cylinder functions of Weber.¹⁵⁻¹⁷ Hence, following Goldstein and Rice,¹³ the new independent variable ξ and dependent variable U are defined by

$$\xi \equiv \sqrt{\frac{2i}{M'k}} \left(\frac{\omega}{c_0} - kM \right) \quad (\text{A11})$$

and

$$P \equiv \frac{e^{b\xi^2/2}}{\frac{1}{2} + b} \frac{d}{d\xi} (e^{-b\xi^2/2} U) \quad (\text{A12})$$

where

$$b \equiv k/2iM' \quad (\text{A13})$$

and

$$M' = -M_0/\delta$$

These transformations are introduced into Eq. (A3), which is then integrated once as in Ref. 13 to obtain Weber's equation:

$$U'' - (\frac{1}{4}\xi^2 + b)U = 0 \quad (\text{A14})$$

where the primes now denote differentiation with respect to ξ . This equation has as its solutions an arbitrary linear combination of parabolic cylinder functions $U(b, \pm\xi)$.¹⁵ Thus, the solution to Eq. (A3) is written as an arbitrary linear combination

$$P = C_+(k) P^+(\xi) + C_-(k) P^-(\xi) \quad (\text{A15})$$

of the functions

$$P^\pm(\xi) = \frac{[U'(b, \pm\xi) \mp b\xi U(b, \pm\xi)]}{\frac{1}{2} + b} \quad (\text{A16})$$

or

$$P^\pm(\xi) = -U(b-l, \pm\xi) + (b-\frac{1}{2})U(b+l, \pm\xi) \quad (\text{A17})$$

Having obtained these solutions [Eqs. (A7, A9, and A15)], the boundary conditions [Eqs. (A5) and (A6)] are applied at the edges of the shear layer to evaluate the coefficient, $A(k)$ in the far-field pressure expression [Eqs. (A7)] as follows:

$$A(k) = \frac{e^{-\gamma_2(-\delta+h)}}{2\pi} \frac{[P^+(\xi_1)P'^-(\xi_1) - P'^+(\xi_1)P^-(\xi_1)]}{G^-R^+ - G^+R^-} \quad (\text{A18})$$

where

$$G^\pm = P'^\pm(\xi_2) - \gamma_2 P^\pm(\xi_2) \quad (\text{A19})$$

$$R^\pm = P'^\pm(\xi_1) + \gamma_1 P^\pm(\xi_1) \quad (\text{A20})$$

and

$$P'^\pm(\xi_i) = \frac{dP^\pm(\xi)}{d\xi} \frac{d\xi}{dy} \Big|_{\xi=\xi_i} \quad i=1,2 \quad (\text{A21})$$

$$\frac{d\xi}{dy} = -\sqrt{2ikM'}$$

where

$$\xi = \xi_1 = \sqrt{\frac{2i}{M'k}} \left(\frac{\omega}{c_0} \right) \quad \text{at } y=0$$

and

$$\xi = \xi_2 = \sqrt{\frac{2i}{M'k}} \left(\frac{\omega}{c_0} - kM_0 \right) \quad \text{at } y=-\delta$$

Putting the appropriate expressions for γ_2 and for $P^\pm(\xi_1)$ and $P'^\pm(\xi_1)$ in the numerator of Eq. (A18) yields,

$$A(k) = 2\exp[-\sqrt{k^2 - [(\omega/c_0) - kM_0]^2}(-\delta+h)] \left(\frac{\omega}{c_0} \right)^2 \times \frac{\sqrt{(i\delta/\pi M_0 k)/[(b+\frac{1}{2})\Gamma(b-\frac{1}{2})]}}{G^-R^+ - G^+R^-} \quad (\text{A22})$$

This expression for $A(k)$ can be put into Eq. (A7) for P_1 , which is the Fourier transform solution for the far-field pressure pattern in region 1. The actual pressure is then obtained from the Fourier inversion integral

$$p_1(x, y) = e^{i\omega t} \int_{-\infty}^{\infty} A(k) \exp[-(ikx + \gamma_1 y)] dk \quad (\text{A23})$$

with $A(k)$ given by Eq. (A22). The preceding integral is of the form

$$\int_{-\infty}^{\infty} g(k) e^{-f(k)} dk$$

where

$$f(k) = ikx + \gamma_1 y \quad (\text{A24})$$

with γ_1 defined by Eq. (A8). This type of integral can be evaluated by the method of stationary phase or saddle point method^{18,19} [for large positive $r=\sqrt{x^2+y^2}$]. The details of the evaluation of Eq. (A23) are presented in Ref. 12. The result is Eq. (6) of the text.

References

- ¹Ribner, H. S., "Reflection, Transmission and Amplification of Sound by a Moving Medium," *Journal of the Acoustical Society of America*, Vol. 29, April 1957, pp. 435-441.
- ²Miles, J. W., "On the Reflection of Sound at an Interface of Relative Motion," *Journal of the Acoustical Society of America*, Vol. 29, Feb. 1957, pp. 226-228.
- ³Gottlieb, P., "Sound Source Near a Velocity Discontinuity," *Journal of the Acoustical Society of America*, Vol. 32, Sept. 1960, pp. 1117-1122.
- ⁴Slutsky, S. and Tamagno, J., "Sound Field Distribution About a Jet," General Applied Science Labs., Tech. Rep. 259, (AFSOR TN-1935), Dec. 1961.
- ⁵Moretti, G. and Slutsky, S., "The Noise Field of a Subsonic Jet," General Applied Science Lab., Tech. Rept. 150 (AFSOR TN-59-1310), Nov. 1959.
- ⁶Slutsky, S., "Acoustic Field of a Cylindrical Jet Due to a Distribution of Random Sources of Quadrupoles," General Applied Science Lab., GASL-TR-281 (AFOSR-2455), Feb. 1962.
- ⁷Graham, E. W. and Graham, B. B., "Effect of a Shear Layer on Plane Waves of Sound in a Fluid," *Journal of the Acoustical Society of America*, Vol. 46, 1969, pp. 169-175.
- ⁸Graham, E. W. and Graham, B. B., "The Acoustical Source in a Two Dimensional Jet," Boeing Scientific Research Labs, D1-82-0909, Sept. 1969.
- ⁹Goldstein, M. E., "The Low Frequency Sound from Multipole Sources in Axisymmetric Shear Flows, with Applications to Jet Noise," *Journal of Fluid Mechanics*, Vol. 70, Aug. 1975, pp. 595-604.
- ¹⁰Goldstein, M. E., "The Low Frequency Sound from Multipole Sources in Axisymmetric Shear Flows—Part 2," *Journal of Fluid Mechanics*, Vol. 75, May 1976, pp. 17-29.
- ¹¹Balsa, T. F., "The Far Field of High Frequency Convected Singularities in Sheared Flows, with an Application to Jet Noise Prediction," *Journal of Fluid Mechanics*, Vol. 74, March 1976, pp. 193-208.
- ¹²Scott, J. N., "A Far Field Analysis of the Propagation of Sound Waves from Various Point Sources Through a Linear Shear Layer," Ph.D. Dissertation, Ohio State University, 1977.
- ¹³Goldstein, M. and Rice, E., "Effect of Shear on Duct Wall Impedance," *Journal of Sound and Vibration*, Vol. 30, Sept. 1973, pp. 79-84.
- ¹⁴Goldstein, M. E., *Aeroacoustics*, McGraw-Hill, New York, 1976.
- ¹⁵Abramowitz, M. and Stegun, I. A., *Handbook of Mathematical Functions with Formulas, Graphs, and Mathematical Tables, National Bureau of Standards Applied Mathematics Series 55*, 1964.
- ¹⁶Olver, F.W.J., "Uniform Asymptotic Expansions for Weber Parabolic Cylinder Functions of Large Order," *Journal of Research NBS*, Vol. 63B, Oct.-Dec. 1959, pp. 131-169.
- ¹⁷Whittaker, E. T. and Watson, G. N., *A Course of Modern Analysis*, 4th ed., Cambridge University Press, Cambridge, England, 1952.
- ¹⁸Erdelyi, A., *Asymptotic Expansions*, Dover Publications, Inc., 1956.
- ¹⁹Carrier, G. F., *Functions of a Complex Variable*, McGraw-Hill, New York, 1966.

From the AIAA Progress in Astronautics and Aeronautics Series...

EXPERIMENTAL DIAGNOSTICS IN GAS PHASE COMBUSTION SYSTEMS—v. 53

*Editor: Ben T. Zinn; Associate Editors: Craig T. Bowman,
Daniel L. Hartley, Edward W. Price, and James F. Skifstad*

Our scientific understanding of combustion systems has progressed in the past only as rapidly as penetrating experimental techniques were discovered to clarify the details of the elemental processes of such systems. Prior to 1950, existing understanding about the nature of flame and combustion systems centered in the field of chemical kinetics and thermodynamics. This situation is not surprising since the relatively advanced states of these areas could be directly related to earlier developments by chemists in experimental chemical kinetics. However, modern problems in combustion are not simple ones, and they involve much more than chemistry. The important problems of today often involve nonsteady phenomena, diffusional processes among initially unmixed reactants, and heterogeneous solid-liquid-gas reactions. To clarify the innermost details of such complex systems required the development of new experimental tools. Advances in the development of novel methods have been made steadily during the twenty-five years since 1950, based in large measure on fortuitous advances in the physical sciences occurring at the same time. The diagnostic methods described in this volume—and the methods to be presented in a second volume on combustion experimentation now in preparation—were largely undeveloped a decade ago. These powerful methods make possible a far deeper understanding of the complex processes of combustion than we had thought possible only a short time ago. This book has been planned as a means of disseminating to a wide audience of research and development engineers the techniques that had heretofore been known mainly to specialists.

671 pp., 6x9, illus., \$20.00/Member \$37.00 List

TO ORDER WRITE: Publications Dept., AIAA, 1290 Avenue of the Americas, New York, N.Y. 10019